

## Quasiparticle properties of the electron gas at metallic densities in the effective-potential expansion method

Yasutami Takada

*Institute for Solid State Physics, University of Tokyo, 7-22-1 Roppongi, Minato-ku, Tokyo 106, Japan*

(Received 16 July 1990)

An extension of the effective-potential expansion method is made to treat low-lying excited states in an interacting many-electron system. This extension provides a prescription for the microscopic calculation of the Landau's Fermi-liquid parameters. By a systematic evaluation of those parameters for the electron gas at metallic densities, we obtain results for the compressibility that are very close to the exact values. We also obtain the results for the spin susceptibility and the effective mass. Those results are compared with those obtained by other methods.

### I. INTRODUCTION

The effective-potential expansion (EPX) method<sup>1</sup> has been applied very successfully to the ground-state properties of the electron gas at metallic densities.<sup>2,3</sup> In the present paper we treat its low-lying excited states using the same method and calculate Landau's Fermi-liquid parameters<sup>4</sup> from first principles to obtain the quasiparticle properties such as the compressibility  $\kappa$ , spin susceptibility  $\chi$ , and effective mass  $m^*$ . Since many calculations have been done for those quantities, we mention first both our ultimate goal and the superiority of our method over others in order to justify yet another calculation on the electron gas.

In spite of the practical usefulness of the density-functional theory (DFT) in the local-density approximation (LDA),<sup>5</sup> many attempts have been made to improve on the DFT-LDA.<sup>6</sup> They are made mostly in the framework of the DFT, but an approach outside the DFT may be necessary to treat strongly correlated systems such as the high- $T_c$  copper oxide superconductors.<sup>7</sup> The main problem in the DFT is the absence of a prescription to calculate the so-called exchange-correlation energy  $E_{xc}$ . DFT-LDA employs the results of  $E_{xc}$  of the electron gas obtained by other methods such as the Green's-function Monte Carlo (GFMC) method.<sup>8,9</sup> Thus a new approach to replace the DFT is required to have such a prescription in a self-contained manner. Before the approach is applied to real solids, its validity should be checked by the calculation of the electronic properties of the electron gas.

About two decades ago, Hedin and Lundqvist<sup>10,11</sup> discussed an approach which might supersede the DFT. In fact, among all the many-body theories associated with the concept of the band structure only their approach has been applied to real metals.<sup>12,13</sup> Its basic idea is due to Hedin,<sup>11</sup> who rearranged the perturbation series in the bare Coulomb potential  $V$  for the electron gas into an expansion in an effective potential  $W$  based on a variational principle. The expansion was successful to some extent.

Its lowest order, or the so-called  $GW$  approximation, gave useful results on the correlation effect.

Unfortunately, however, Hedin's theory is not a particularly good one for the electron gas relative to the present standard of many-body theories. Many-body effects in the electron gas cannot be treated satisfactorily unless we include appropriate sums of the ring, exchange, and ladder diagrams for the processes of the momentum transfer  $q$  in the regions of  $q \approx 0$ ,  $q \approx k_F$ , and  $q \geq 2k_F$ , respectively, in the language of the perturbation-theoretic approach,<sup>14</sup> where  $k_F$  is the Fermi momentum. In Hedin's theory the ring diagrams are included completely through the random-phase approximation (RPA),<sup>15</sup> but other diagrams are neglected in the  $GW$  approximation or they are treated very crudely in the next-order approximation.<sup>12</sup>

The EPX method is conceptually very similar to Hedin's theory, but there is an important difference in the choice of an expansion parameter. Hedin chose the dynamically screened Coulomb potential  $W(q, \omega)$ , where  $\omega$  is the energy transfer. His choice, however, is not good enough for the quantitative purpose as seen by the fact that the  $GW$  approximation<sup>11</sup> as well as an improvement on it by the inclusion of some next-order terms<sup>12</sup> gave a ground-state energy lower than the more accurate one obtained in GFMC calculations. Since Hedin's expansion in  $W$  is based on a variational principle, the energy obtained must be larger than the exact energy, if the convergence of the series is good enough. The violation of the upper-bound property for the ground-state energy indicates that his series should not be cut off at such low orders as the first or second. In fact,  $W(q, \omega)$  has a plasmon pole, and thus it becomes very large in some region in the  $(q, \omega)$  plane. On the other hand, the EPX method is formulated in terms of the static potential  $W(q, 0)$  or  $\tilde{V}$  in its notation. This is a very good expansion parameter, and the upper-bound property holds in the EPX method.<sup>2,16</sup>

In Hedin's theory, it is not easy in practice to go beyond the  $GW$  approximation, because not a simplification, but only a rearrangement of terms is done

in the usual perturbation expansion. In the EPX method, however, a considerable simplification is made by the choice of a very simple, but physically acceptable, trial many-body wave function. Thus we can rather easily perform higher-order calculations for a systematic improvement.

Let us now compare the EPX method with the perturbation-theoretic and equation-of-motion methods,<sup>17</sup> which have been most often used to calculate  $\kappa$ ,  $\chi$ , and  $m^*$  of the electron gas. In those methods the so-called local-field correction  $G(q)$  is always introduced to treat the vertex corrections which come from the exchange and ladder diagrams. It is true that  $G(q)$  is useful for a qualitative understanding of the exchange and correlation effects,<sup>18</sup> but we have to realize that this is only an approximate treatment. We can never expect that all the vertex corrections are written only as a function of  $q$ . Besides, the best choice for  $G(q)$  depends on the channel. Namely,  $G(q)$  for the electron-electron channel is different from that for the electron-hole channel.<sup>19</sup> Further, when we derive Landau's Fermi-liquid interaction from an expression for the ground-state energy with  $G(q)$  included, special care is necessary for the spin-dependent part.<sup>20</sup> In fact, there are some ambiguities in that treatment and an error has been pointed out.<sup>21</sup> Thus, if possible, it is better to avoid the use of  $G(q)$ . In the EPX method we can do without  $G(q)$ . The vertex corrections in an expansion in  $\tilde{V}$  are calculated faithfully in which the Pauli principle, the  $f$ -sum rule, and Ward's identity<sup>22</sup> are satisfied order by order.

Calculations of  $\kappa$ ,  $\chi$ , and  $m^*$  are also done in the modern variational approach in which the trial function is usually taken in the form of the Jastrow wave function.<sup>23</sup> In this approach the expectation value of the Hamiltonian is evaluated by either the Monte Carlo methods<sup>24,25</sup> or the Fermi hypernetted-chain (FHNC) methods.<sup>26,27</sup> The FHNC methods, combined with the theory of correlated basis functions (CBF),<sup>28</sup> are good enough to provide very accurate correlation energy.<sup>29</sup> But we already know that because of the absence of the energy denominators in the definition of the Jastrow function, we cannot obtain accurate values for the quasiparticle properties near the Fermi surface in the system with the bare interaction having a  $q^{-2}$  singularity at  $q=0$  such as the Coulomb potential.<sup>3</sup> Such energy denominators are included in the trial function in the EPX method.

This paper is organized as follows. In Sec. II we derive the basic formulas for the quasiparticle energy and Landau's Fermi-liquid interaction by making an extension of the EPX method to treat low-lying excited states of an interacting many-electron system. In Sec. III a microscopic expression for Landau's Fermi-liquid interaction is shown. It is given by an expansion series, and all

the terms up to second order are represented diagrammatically. We introduce a static screened interaction as the largest contribution to the spin-parallel Landau interaction function. In Sec. IV we evaluate Landau's Fermi-liquid parameters for the electron gas at metallic densities and obtain our results for  $\kappa$ ,  $\chi$ , and  $m^*$ . Those values are compared with those in other approaches. Summaries of this paper are given in Sec. V. We employ units in which  $\hbar=1$ .

## II. ENERGY FUNCTIONAL

### A. Hamiltonian

The electron gas is a system consisting of  $N$  electrons embedded in a uniform positive-charge background. The electrons interact with one another through the Coulomb interaction. Thus the Hamiltonian is written in second quantization as

$$H = H_0 + V, \quad (2.1)$$

where

$$H_0 = \sum_{\mathbf{k}, \sigma} \epsilon_{\mathbf{k}} C_{\mathbf{k}\sigma}^\dagger C_{\mathbf{k}\sigma} \quad (2.2)$$

and

$$V = \frac{1}{2} \sum_{q(\neq 0)} \sum_{\mathbf{k}, \sigma} \sum_{\mathbf{k}', \sigma'} V(q) C_{\mathbf{k}+\mathbf{q}, \sigma}^\dagger C_{\mathbf{k}'-\mathbf{q}, \sigma'}^\dagger C_{\mathbf{k}'\sigma'} C_{\mathbf{k}\sigma}, \quad (2.3)$$

with  $\epsilon_{\mathbf{k}} = \mathbf{k}^2/2m$  and  $V(q) = 4\pi e^2/q^2$ . The volume of the system is taken to be unity. We specify an electron by momentum  $\mathbf{k}$  and spin  $\sigma$  and represent its annihilation operator by  $C_{\mathbf{k}\sigma}$ . In the following we measure momenta and energies in units of  $k_F$  and rydberg (Ry)  $me^4/2$ , respectively. Then the system is described only by one parameter  $r_s$ , defined by  $r_s \equiv me^2/\alpha k_F$ , with  $\alpha = (4/9\pi)^{1/3} = 0.521$ . In this paper we consider  $r_s$  in the range 1–6.

### B. Trial function and energy for the ground state

In the EPX method a trial function for the ground state is given with a state described by the plane-wave Slater determinant  $|0\rangle$  and a correlation operator  $U(0, -\infty)$  as<sup>16</sup>

$$|\Phi_0\rangle = U(0, -\infty)|0\rangle \equiv \sum_{n=0}^{\infty} \frac{1}{n!} \left[ \sum_{m=1}^{\infty} U_m(0, -\infty) \right]^n |0\rangle, \quad (2.4)$$

where  $U_m(0, -\infty)$  is defined as

$$\begin{aligned} U_m(0, -\infty) &= \frac{(-i)^m}{m!} \int_{-\infty}^0 e^{0^+t_1} dt_1 \cdots \int_{-\infty}^0 e^{0^+t_m} dt_m T[\tilde{V}_l(t_1) \cdots \tilde{V}_l(t_m)]_L \\ &+ \frac{(-i)^m}{(m-1)!} \int_{-\infty}^0 e^{0^+t_1} dt_1 \cdots \int_{-\infty}^0 e^{0^+t_m} dt_m T[\tilde{V}_s(t_1) \tilde{V}_l(t_2) \cdots \tilde{V}_l(t_m)]_L, \end{aligned} \quad (2.5)$$

with the long- and short-range parts of the effective potential  $\bar{V}_l$  and  $\bar{V}_s$ . We do not explain either the meanings of the symbols in (2.5) or the physical considerations to reach this form. Both of them were given in detail in Ref. 16, which will be referred to as I hereafter.

We can write the energy expectation value  $E_0$  with respect to  $|\Phi_0\rangle$  as a power series in  $\bar{V}_s$  as

$$E_0 \equiv \frac{\langle \Phi_0 | H | \Phi_0 \rangle}{\langle \Phi_0 | \Phi_0 \rangle} = \sum_{n=0}^{\infty} E^{(n)}. \quad (2.6)$$

The  $n$ th-order term in (2.6) is given by the sum of the terms, each of which is represented as a multidimensional integral of momentum variables for the integrand composed of several  $n_{k\sigma}$ 's,  $n\bar{V}_s(q)$ 's, and numbers of  $\bar{V}_l(q)$ 's up to infinite order. Here  $n_{k\sigma}$  is the distribution functions of a free-electron system, i.e.,  $\theta(k_F - |\mathbf{k}|)$ , and  $\bar{V}_s(q)$  is given by

$$\bar{V}_s(q) \equiv \frac{\bar{V}_s(q)}{[\epsilon(q, 0)]^2}, \quad (2.7)$$

with the dielectric function  $\epsilon(q, \Omega)$ , defined through the polarization function  $\Pi(q, \Omega)$  in the RPA as

$$\epsilon(q, \Omega) = 1 + \Pi(q, \Omega)\bar{V}_l(q). \quad (2.8)$$

Thus we may regard  $E_0$  as a functional of those functions:

$$E_0 = E_0\{\bar{V}_l(q), \bar{V}_s(q), n_{k\sigma}\}. \quad (2.9)$$

Since all the important terms in  $E_0$  up to eighth order were given explicitly in I, this functional is essentially a known quantity to us.

In I we determined the optimum values for  $\bar{V}_l(q)$  and  $\bar{V}_s(q)$  by changing them in (2.9) with  $n_{k\sigma}$  fixed to  $\theta(k_F - |\mathbf{k}|)$ . The obtained results for the optimum  $\bar{V}_l(q)$  and  $\bar{V}_s(q)$  were shown in Fig. 5 in I. We note that  $\bar{V}_l(q)$  is not zero only for small  $q$ ; i.e.,  $q$  less than about  $0.2k_F$ , while  $\bar{V}_s(q)$  is very small in that region.

### C. Trial function and energy for low-lying excited states

In the absence of the interaction, all the excited states are given by the addition of electrons to and/or the subtraction of them from  $|0\rangle$ , i.e.,

$$C_{k\sigma}^\dagger C_{k'\sigma'}^\dagger \cdots C_{p\tau} C_{p'\tau'} \cdots |0\rangle \quad \text{for } |\mathbf{k}|, |\mathbf{k}'|, \dots > k_F$$

and  $|\mathbf{p}|, |\mathbf{p}'|, \dots < k_F$ . In the presence of the interaction, we follow Landau's conjecture<sup>4</sup> and write the trial function for low-lying excited states as

$$|\Phi_{k\sigma k'\sigma' \dots; p\tau p'\tau' \dots}\rangle = U(0, -\infty) C_{k\sigma}^\dagger C_{k'\sigma'}^\dagger \cdots C_{p\tau} C_{p'\tau'} \cdots |0\rangle, \quad (2.10)$$

in which  $U(0, -\infty)$  is the same as in (2.4).

The excitation energy  $\bar{\epsilon}_{k\sigma}$  for the state  $|\Phi_{k\sigma}\rangle$  with  $|\mathbf{k}| > k_F$  is given by the difference between the energy expectation value with respect to  $|\Phi_{k\sigma}\rangle$  and the ground-state energy  $E_0$ :

$$\bar{\epsilon}_{k\sigma} \equiv \frac{\langle \Phi_{k\sigma} | H | \Phi_{k\sigma} \rangle}{\langle \Phi_{k\sigma} | \Phi_{k\sigma} \rangle} - E_0. \quad (2.11)$$

We can calculate the first term in (2.11) in a method similar to that in (2.6). Namely, compared to the calculation of  $E_0$ , we only need to consider the existence of an extra electron at  $\mathbf{k}$  in addition to the Fermi sphere. This change of the electron configuration in the noninteracting system can be included in the energy calculation by that of the occupation number  $n_{k\sigma}$  as explained by Gell-Mann<sup>30</sup> in the calculation of the specific heat of the electron gas at high densities. Then the argument in Ref. 30 shows clearly that  $\bar{\epsilon}_{k\sigma}$  is given by

$$\bar{\epsilon}_{k\sigma} = \frac{\delta E_0\{\bar{V}_l(q), \bar{V}_s(q), n_{k\sigma}\}}{\delta n_{k\sigma}}. \quad (2.12)$$

The same is found to hold even for  $|\mathbf{k}| < k_F$ . Note that in (2.12) both  $\bar{V}_l(q)$  and  $\bar{V}_s(q)$  are kept fixed, because  $U(0, -\infty)$  is fixed to its ground-state value in (2.10). Actually, even if they are not fixed, there is no change in the result of (2.12), because those functions are chosen to give the optimum value for  $E_0$ , and thus the derivatives of  $E_0$  with respect to them vanish. The above argument explains the reason why the correlation factor  $U(0, -\infty)$  in (2.10) is chosen to be equal to that for the ground state from the outset. The same situation always occurs in the variational treatments.<sup>29,31</sup>

The interaction energy  $f_{k\sigma k'\sigma'}$  between the two quasiparticles specified by  $k\sigma$  and  $k'\sigma'$  with  $|\mathbf{k}|, |\mathbf{k}'| > k_F$  can be defined as

$$f_{k\sigma k'\sigma'} \equiv \frac{\langle \Phi_{k\sigma k'\sigma'} | H | \Phi_{k\sigma k'\sigma'} \rangle}{\langle \Phi_{k\sigma k'\sigma'} | \Phi_{k\sigma k'\sigma'} \rangle} - E_0 - \bar{\epsilon}_{k\sigma} - \bar{\epsilon}_{k'\sigma'}. \quad (2.13)$$

By a similar argument leading to (2.12) from (2.11), we obtain

$$f_{k\sigma k'\sigma'} = \frac{\delta^2 E_0}{\delta n_{k\sigma} \delta n_{k'\sigma'}}. \quad (2.14)$$

This equation is found to hold even for  $|\mathbf{k}|$  and/or  $|\mathbf{k}'|$  less than  $k_F$ . Thus (2.14) provides the Landau interaction function if both  $|\mathbf{k}|$  and  $|\mathbf{k}'|$  are taken to be equal to  $k_F$ .

To conclude this section, we note that the Fermi-liquid theory is reformulated in the present framework. In particular, the EPX method provides an explicit form for the operator  $U(0, -\infty)$ , by which each of the low-lying excited states in the interacting system is mapped one to one from the corresponding state in the noninteracting system.

### III. FERMI-LIQUID INTERACTION

According to the usual diagrammatic analysis,<sup>32</sup> the Landau interaction function  $f_{k\sigma k'\sigma'}$  satisfies an integral equation which is shown in Fig. 1, where  $z$  is the renormalization factor at the Fermi surface,  $I_{k\sigma k'\sigma'}$  is the irre-

ducible particle-hole interaction, and  $\tilde{G}_{\mathbf{k}\sigma\mathbf{k}'\sigma'}$  is the full Green's function in the interacting system. By taking the functional derivative of (2.14) with  $E_0$  in the expansion (2.6), we obtain an explicit expression for  $f_{\mathbf{k}\sigma\mathbf{k}'\sigma'}$  term by term from zeroth order in a tedious but straightforward way. In the following we show the result of such a calculation. To avoid too many equations in this paper, most of the terms are given only in the diagrammatic form arranged in such a way as in Fig. 1.

### A. Zeroth-order terms

Let us combine the Hartree-Fock terms  $E_{\text{HF}}$  with the ring terms  $E_r^{(0)}(V)$  and  $E_r^{(0)}(H_0)$ , which are shown in Figs. 1(a) and 1(b) in I. Their contribution to the Landau interaction  $f_{\mathbf{k}\sigma\mathbf{k}'\sigma'}^{(0;r)}$  is obtained as

$$f_{\mathbf{k}\sigma\mathbf{k}'\sigma'}^{(0;r)} = -\delta_{\sigma\sigma'} \left[ \bar{V}(|\mathbf{k}-\mathbf{k}'|) + \Pi(|\mathbf{k}-\mathbf{k}'|, 0) \frac{[\tilde{V}_l(|\mathbf{k}-\mathbf{k}'|)]^2}{[\epsilon(|\mathbf{k}-\mathbf{k}'|, 0)]^2} \right] - \sum_q \int_{-\infty}^{\infty} \frac{d\Omega}{2\pi i} \frac{2V(q) - \tilde{V}_l(q) + \Pi(q, \Omega) [\tilde{V}_l(q)]^2}{[\epsilon(q, \Omega)]^3} \tilde{V}_l(q) [G_{\mathbf{k}'+\mathbf{q}, \sigma'}(\Omega) + G_{\mathbf{k}-\mathbf{q}, \sigma'}(-\Omega)] G_{\mathbf{k}+\mathbf{q}, \sigma}(\Omega), \quad (3.1)$$

where  $G_{\mathbf{k}\sigma}(\Omega)$  is the single-particle Green's function in the noninteracting system, and  $\bar{V}(q)$  is defined as

$$\bar{V}(q) \equiv \frac{V(q)}{[\epsilon(q, 0)]^2}. \quad (3.2)$$

Although  $f_{\mathbf{k}\sigma\mathbf{k}'\sigma'}^{(0;r)}$  will be evaluated as it is in (3.1) in Sec. IV, only a small change is found even if we neglect the terms of the order of  $\tilde{V}_l^2/\epsilon^2$  or higher. Thus, for simplicity, only the terms up to first order in  $\tilde{V}_l/\epsilon$  are drawn for  $f_{\mathbf{k}\sigma\mathbf{k}'\sigma'}^{(0;r)}$  in Fig. 2(a). Note also that we did not show those diagrams which can be obtained by the interchange of the two different interaction lines. Namely, only the diagrams having the topologically different structures are given. Simplifications of similar kinds will also be applied to the diagrammatic expressions for other terms in  $f_{\mathbf{k}\sigma\mathbf{k}'\sigma'}$ .

Besides the Hartree-Fock and ring terms, the exchange and self-energy terms [Figs. 1(c) and 1(d) in I] were included in  $E^{(0)}$ . Their contributions to the Landau interaction function are shown diagrammatically in Figs. 2(b) and 2(c) to first order in  $\tilde{V}_l/\epsilon$ . The sum of all those diagrams is found to be negligibly small. The same is true even if we consider the terms up to second order in  $\tilde{V}_l/\epsilon$ . As for the diagrammatic structure in Fig. 2, the diagrams in Figs. 2(a) and 2(b) are examples of the terms in  $I_{\mathbf{k}\sigma\mathbf{k}'\sigma'}$ . Each diagram given in (b<sub>i</sub>) corresponds to that in (a<sub>i</sub>) as an exchange partner. The term (c<sub>1</sub>) provides the contribution of the renormalization factor, and that of (c<sub>2</sub>) is an example of the second diagram of the integral equation for  $f_{\mathbf{k}\sigma\mathbf{k}'\sigma'}$  in Fig. 1. Although we have obtained the terms represented by the diagrams with the self-energy correction in the other part of the electron line in (c<sub>1</sub>), they are suppressed for simplicity. Note also that the contribution from the diagram given by the interchange of  $\bar{V}$  with  $\tilde{V}_l/\epsilon$  in (c<sub>1</sub>) vanishes if we neglect the  $\Omega$  dependence in  $\bar{V}$ . Even if we include the  $\Omega$  dependence, its contribution is very small.

### B. First-order terms

The contribution from the first-order ring terms [Figs. 3(a<sub>1</sub>) and (a<sub>2</sub>) in I] is given as

$$f_{\mathbf{k}\sigma\mathbf{k}'\sigma'}^{(1;r)} = 2\delta_{\sigma\sigma'} \frac{[V(|\mathbf{k}-\mathbf{k}'|) - \tilde{V}_l(|\mathbf{k}-\mathbf{k}'|)] \tilde{V}_s(|\mathbf{k}-\mathbf{k}'|) \Pi(|\mathbf{k}-\mathbf{k}'|, 0)}{[\epsilon(|\mathbf{k}-\mathbf{k}'|, 0)]^3} - 2 \sum_q \int_{-\infty}^{\infty} \frac{d\Omega}{2\pi i} \frac{[V(q) - \tilde{V}_l(q)] \tilde{V}_s(q)}{[\epsilon(q, \Omega)]^3} \left[ 1 - 3 \frac{\Pi(q, \Omega) \tilde{V}_l(q)}{\epsilon(q, \Omega)} \right] [G_{\mathbf{k}'+\mathbf{q}, \sigma'}(\Omega) + G_{\mathbf{k}-\mathbf{q}, \sigma'}(-\Omega)] G_{\mathbf{k}+\mathbf{q}, \sigma}(\Omega). \quad (3.3)$$

Since the product of  $\tilde{V}_s(q)$  with  $\tilde{V}_l(q)/\epsilon(q, 0)$  becomes very small as mentioned at the end of Sec. II B, we can neglect the terms having at least one such product. Then we can perform the  $\Omega$  integral in (3.3) to obtain

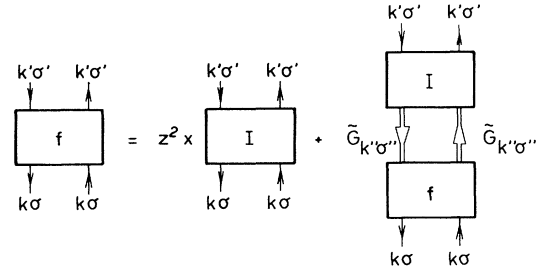


FIG. 1. Integral equation to determine the Landau interaction function  $f_{\mathbf{k}\sigma\mathbf{k}'\sigma'}$  in terms of the so-called irreducible electron-hole interaction  $I_{\mathbf{k}\sigma\mathbf{k}'\sigma'}$  and full Green's function in the interacting system  $\tilde{G}_{\mathbf{k}\sigma\mathbf{k}'\sigma'}$ . In the formal analysis,  $I_{\mathbf{k}\sigma\mathbf{k}'\sigma'}$  should be multiplied by  $z^2$  in the first term to obtain  $f_{\mathbf{k}\sigma\mathbf{k}'\sigma'}$ , where  $z$  is the renormalization factor at the Fermi surface.

$$\begin{aligned}
f_{k\sigma k'\sigma'}^{(1:r)} &= 2\delta_{\sigma\sigma'} \bar{V}(|\mathbf{k}-\mathbf{k}'|) \bar{V}_s(|\mathbf{k}-\mathbf{k}'|) \epsilon(|\mathbf{k}-\mathbf{k}'|, 0) \Pi(|\mathbf{k}-\mathbf{k}'|, 0) \\
&+ 2 \sum_{\mathbf{q}} \bar{V}(q) \bar{V}_s(q) \left[ \frac{n_{\mathbf{k}+\mathbf{q}\sigma}(1-n_{\mathbf{k}'+\mathbf{q}\sigma'})}{\epsilon_{\mathbf{k}'+\mathbf{q}} - \epsilon_{\mathbf{k}+\mathbf{q}}} + \frac{n_{\mathbf{k}'+\mathbf{q}\sigma'}(1-n_{\mathbf{k}+\mathbf{q}\sigma})}{\epsilon_{\mathbf{k}+\mathbf{q}} - \epsilon_{\mathbf{k}'+\mathbf{q}}} \right. \\
&\quad \left. - \frac{(1-n_{\mathbf{k}+\mathbf{q}\sigma})(1-n_{\mathbf{k}'-\mathbf{q}\sigma'})}{\epsilon_{\mathbf{k}+\mathbf{q}} + \epsilon_{\mathbf{k}'-\mathbf{q}} - 2\epsilon_F} - \frac{n_{\mathbf{k}+\mathbf{q}\sigma} n_{\mathbf{k}'-\mathbf{q}\sigma'}}{2\epsilon_F - \epsilon_{\mathbf{k}+\mathbf{q}} - \epsilon_{\mathbf{k}'-\mathbf{q}}} \right], \quad (3.4)
\end{aligned}$$

where  $\epsilon_F$  is the Fermi energy  $k_F^2/2m$ . The terms in  $f_{k\sigma k'\sigma'}^{(1:r)}$  are shown diagrammatically in Fig. 3(a). The first term in (3.4) is represented in (a<sub>1</sub>), in which we can neglect an extra factor of  $\epsilon(|\mathbf{k}-\mathbf{k}'|, 0)$  because it gives rise to the contribution higher than first order in  $\bar{V}_l/\epsilon$ . The first two terms in the square bracket give the contribution from the electron-hole scatterings as shown in (a<sub>2</sub>), while the third and fourth terms give, respectively, those from the electron-electron and the hole-hole scatterings as shown in (a<sub>3</sub>).

A similar calculation is done for the exchange term  $E_{\text{ex}}^{(1)}(V)$  [Fig. 3(b<sub>1</sub>) in I], and the result is given as

$$\begin{aligned}
f_{k\sigma k'\sigma'}^{(1:\text{ex})} &= -2\delta_{\sigma\sigma'} \bar{V}_s(|\mathbf{k}-\mathbf{k}'|) \sum_{\mathbf{p}} [\bar{V}(|\mathbf{k}'-\mathbf{p}|) + \bar{V}(|\mathbf{k}+\mathbf{p}|)] \frac{n_{\mathbf{p}\sigma}(1-n_{\mathbf{p}+\mathbf{k}-\mathbf{k}',\sigma})}{\epsilon_{\mathbf{p}+\mathbf{k}-\mathbf{k}'} - \epsilon_{\mathbf{p}}} \\
&- 2\delta_{\sigma\sigma'} \sum_{\mathbf{q}} \bar{V}_s(q) \left[ \bar{V}(|\mathbf{k}'-\mathbf{k}|) \left[ \frac{n_{\mathbf{k}+\mathbf{q},\sigma}(1-n_{\mathbf{k}'+\mathbf{q},\sigma'})}{\epsilon_{\mathbf{k}'+\mathbf{q}} - \epsilon_{\mathbf{k}+\mathbf{q}}} + \frac{n_{\mathbf{k}'+\mathbf{q},\sigma'}(1-n_{\mathbf{k}+\mathbf{q},\sigma})}{\epsilon_{\mathbf{k}+\mathbf{q}} - \epsilon_{\mathbf{k}'+\mathbf{q}}} \right] \right. \\
&\quad \left. - \bar{V}(|\mathbf{k}'-\mathbf{k}-\mathbf{q}|) \left[ \frac{(1-n_{\mathbf{k}+\mathbf{q},\sigma})(1-n_{\mathbf{k}'-\mathbf{q},\sigma'})}{\epsilon_{\mathbf{k}+\mathbf{q}} + \epsilon_{\mathbf{k}'-\mathbf{q}} - 2\epsilon_F} + \frac{n_{\mathbf{k}+\mathbf{q},\sigma} n_{\mathbf{k}'-\mathbf{q},\sigma'}}{2\epsilon_F - \epsilon_{\mathbf{k}+\mathbf{q}} - \epsilon_{\mathbf{k}'-\mathbf{q}}} \right] \right]. \quad (3.5)
\end{aligned}$$

Diagrammatic representations for the terms in (3.5) are given in Fig. 3(b). As in Fig. 2, the term (b<sub>i</sub>) is an exchange partner to that in (a<sub>i</sub>).

Other diagrams for  $E^{(1)}$  considered in Fig. 3 in I also give contributions to the Landau interaction function to first order, but the sum of those contributions is found to be very small. Thus we do not write those terms explicitly here. Note, however, that their contribution is included in the final results for  $\kappa$ ,  $\chi$ , and  $m^*$  in Sec. IV.

### C. Second-order $H_0$ terms

The terms in  $E^{(2)}(H_0)$  [Fig. 4(a) in I] are structurally the same as those in the first-order ring and exchange diagrams. Thus their contribution to the Landau interaction function is readily calculated to give  $f_{k\sigma k'\sigma'}^{(2:H_0)}$  by the sum of (3.4) and (3.5) with the replacement of  $2\bar{V}$  by  $-\bar{V}_s$ . We suppress the diagrams for  $f_{k\sigma k'\sigma'}^{(2:H_0)}$ , because they are almost the same as those for  $f_{k\sigma k'\sigma'}^{(1:r)}$  and  $f_{k\sigma k'\sigma'}^{(1:\text{ex})}$ .

### D. Second-order ring and ladder families

Among the second-order terms, the ring and the ladder families [Figs. 4(b) and 4(d) in I] provide many complicated diagrams for  $I_{k\sigma k'\sigma'}$ . Diagrammatically, the Landau interaction function is given by cuts of the two electron lines in all the possible ways in the diagrams to express the energy functional. We divide the contributions from the ring family into two classes. One is the sum of the terms given by the successive cuts of the electron lines in the same electronic polarization bubble in the ring diagram and those given by exactly the same cut in the corresponding exchange diagrams. We call the contribution the second-order static screened interaction  $f_{k\sigma k'\sigma'}^{(2:rs)}$ . In our definition the static screened interactions in zeroth and first orders are given by the sum of (a<sub>1</sub>) and (b<sub>1</sub>) in Figs. 2 and 3, respectively, and they are represented by  $f_{k\sigma k'\sigma'}^{(0:rs)}$  and  $f_{k\sigma k'\sigma'}^{(1:rs)}$ . The corresponding term in  $f_{k\sigma k'\sigma'}^{(2:H_0)}$  will be written as  $f_{k\sigma k'\sigma'}^{(2:H_0;rs)}$ . The terms in  $f_{k\sigma k'\sigma'}^{(2:rs)}$  are shown in Fig. 4(a) and are obtained as

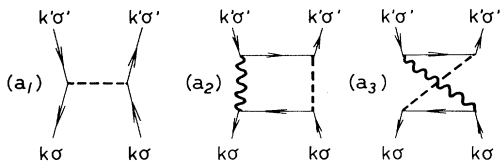
$$\begin{aligned}
f_{k\sigma k'\sigma'}^{(2:rs)} = & -2\delta_{\sigma\sigma'} \bar{V}_s(|\mathbf{k}-\mathbf{k}'|) \sum_{\mathbf{p},\tau} \sum_{\mathbf{p}',\tau'} \left[ \{ \bar{V}_s(|\mathbf{k}-\mathbf{k}'|) [V(|\mathbf{k}'-\mathbf{k}|) - \delta_{\tau\tau'} \bar{V}(|\mathbf{p}'-\mathbf{p}|)] \right. \\
& - \delta_{\tau\sigma} [\bar{V}(|\mathbf{k}'-\mathbf{k}|)\epsilon(|\mathbf{k}'-\mathbf{k}|,0) - \delta_{\tau\tau'} \bar{V}(|\mathbf{p}'-\mathbf{p}|)] [\bar{V}_s(|\mathbf{p}-\mathbf{k}'|) + \bar{V}_s(|\mathbf{p}+\mathbf{k}|)] \} \\
& \times \frac{n_{\mathbf{p}\tau}(1-n_{\mathbf{p}+\mathbf{k}-\mathbf{k}',\tau})}{\epsilon_{\mathbf{p}+\mathbf{k}-\mathbf{k}'-\epsilon_{\mathbf{p}}} \frac{n_{\mathbf{p}'\tau'}(1-n_{\mathbf{p}'+\mathbf{k}-\mathbf{k}',\tau'})}{\epsilon_{\mathbf{p}'+\mathbf{k}-\mathbf{k}'-\epsilon_{\mathbf{p}'}}} \\
& + (\bar{V}_s(|\mathbf{k}-\mathbf{k}'|) \{ 2V(|\mathbf{k}'-\mathbf{k}|) - \delta_{\sigma\tau'} \epsilon(|\mathbf{k}-\mathbf{k}',0) [\bar{V}(|\mathbf{k}+\mathbf{p}'|) + \bar{V}(|\mathbf{k}'-\mathbf{p}'|)] \} \\
& - \delta_{\tau\tau'} \bar{V}_s(|\mathbf{p}'+\mathbf{p}-\mathbf{k}'+\mathbf{k}|) \{ 2\bar{V}(|\mathbf{k}'-\mathbf{k}|) - \delta_{\tau\sigma} [\bar{V}(|\mathbf{k}+\mathbf{p}'|) + \bar{V}(|\mathbf{k}'-\mathbf{p}'|)] \} \\
& - \delta_{\sigma\tau} \{ \bar{V}(|\mathbf{k}'-\mathbf{k}|)\epsilon(|\mathbf{k}'-\mathbf{k}|,0) [\bar{V}_s(|\mathbf{p}-\mathbf{k}'|) + \bar{V}_s(|\mathbf{p}+\mathbf{k}|)] \\
& - \delta_{\sigma\tau'} [\bar{V}(|\mathbf{k}+\mathbf{p}'|) \bar{V}_s(|\mathbf{p}-\mathbf{k}'|) + \bar{V}(|\mathbf{k}'-\mathbf{p}'|) \bar{V}_s(|\mathbf{p}+\mathbf{k}|)] \} \} \\
& \times \frac{n_{\mathbf{p}\tau}(1-n_{\mathbf{p}+\mathbf{k}-\mathbf{k}',\tau})}{\epsilon_{\mathbf{p}+\mathbf{k}-\mathbf{k}'-\epsilon_{\mathbf{p}}} \frac{n_{\mathbf{p}'\tau'}(1-n_{\mathbf{p}'+\mathbf{k}-\mathbf{k}',\tau'})}{\epsilon_{\mathbf{p}'+\mathbf{k}-\mathbf{k}'-\epsilon_{\mathbf{p}'} + \epsilon_{\mathbf{p}+\mathbf{k}-\mathbf{k}'-\epsilon_{\mathbf{p}}}} \Big]. \quad (3.6)
\end{aligned}$$

Other terms derived from the energy functional in the ring family constitute another class of the Landau interaction. Since those terms involve the dynamic scattering process of either electron-electron, hole-hole, or electron-hole, we call the contribution the dynamic interaction  $f_{k\sigma k'\sigma'}^{(2:rd)}$ . In a similar way we can define  $f_{k\sigma k'\sigma'}^{(0:rd)}$ ,  $f_{k\sigma k'\sigma'}^{(1:rd)}$ , and  $f_{k\sigma k'\sigma'}^{(2:H_0;rd)}$ . In Figs. 4(b) and 4(c) the diagrams for  $f_{k\sigma k'\sigma'}^{(2:rd)}$  and the contributions from the ladder family  $f_{k\sigma k'\sigma'}^{(2:l)}$  are shown. Explicit representations for those

terms are too long to show here. Note that the terms (b<sub>1</sub>)–(b<sub>10</sub>) and (c<sub>1</sub>)–(c<sub>8</sub>) give the components of the spin-independent interaction, while other terms work only between the electrons with parallel spins.

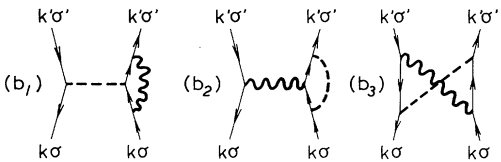
The idea to separate  $f_{k\sigma k'\sigma'}^{(2:rs)}$  from other second-order terms is inspired by the discussion of Yasuhara, Ousaka, and Suehiro.<sup>21</sup> They paid special attention to the class of diagrams in  $I_{k\sigma k'\sigma'}$ , which can be divided into two parts by the cut of one interaction line with the momentum transfer  $\mathbf{k}'-\mathbf{k}$ . However, the sum of such diagrams,  $f_{k\sigma k'\sigma'}^{(sc)}$ , is not the same as the static screened interaction in our definition, because the terms (b<sub>11</sub>), (b<sub>13</sub>), (b<sub>15</sub>), (b<sub>19</sub>), (c<sub>9</sub>)–(c<sub>16</sub>), and (c<sub>24</sub>) in Fig. 4 are not included in  $f_{k\sigma k'\sigma'}^{(2:rs)}$ . This difference comes from that of the basic principle to classify the diagrams: Our main concern is to treat the direct and exchange terms in pairs. Thus, as long as its direct (or exchange) partner is involved in either  $f_{k\sigma k'\sigma'}^{(2:rd)}$

(a) Contribution from Fock and Ring Terms



where ---- =  $V/\epsilon^2$  and  $\sim\sim\sim = \tilde{V}_l/\epsilon$

(b) Contribution from Exchange Term



(c) Contribution from Self-Energy Term

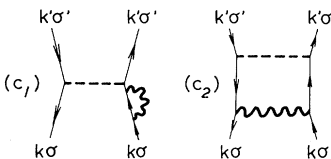
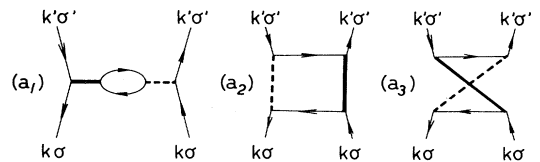


FIG. 2. Diagrammatic representation for  $f_{k\sigma k'\sigma'}$  to first order in  $\tilde{V}_l/\epsilon$  and in zeroth order in  $\bar{V}_s$ . The contributions from the ring, including the Fock diagram, exchange, and self-energy terms, are, respectively, shown in (a), (b), and (c).

(a) Contribution from Ring Terms



where ---- =  $\tilde{V}_s/\epsilon^2$

(b) Contribution from Exchange Term

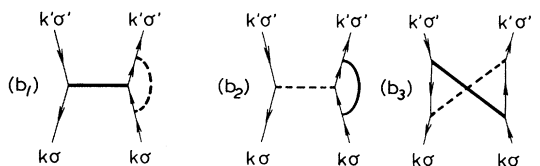


FIG. 3. Diagrammatic representation for  $f_{k\sigma k'\sigma'}$  in first order in  $\bar{V}_s$ . Those terms are classified into (a) the ring and (b) the exchange contributions.

or  $f_{k\sigma k'\sigma'}^{(2;1)}$ , we include its exchange (or direct) counterpart in the same class even if its structure may be classified as the static screened interaction in the definition of Ref. 21. In fact, our choice is superior to that in Ref. 21, because  $f_{k\sigma k'\sigma'}^{(sc)}$  has an unphysical divergence which can be suppressed only when the corresponding divergence in other terms in  $I_{k\sigma k'\sigma'}$  is added to it.<sup>33</sup> Such an unphysical

divergence does not appear in our static screened interaction.

### E. Second-order self-energy family

As in the zeroth-order terms in Fig. 2(c), the self-energy diagrams [Fig. 4(c) in I] give the terms in the Landau interaction function  $f_{k\sigma k'\sigma'}^{(2;s)}$  structurally very

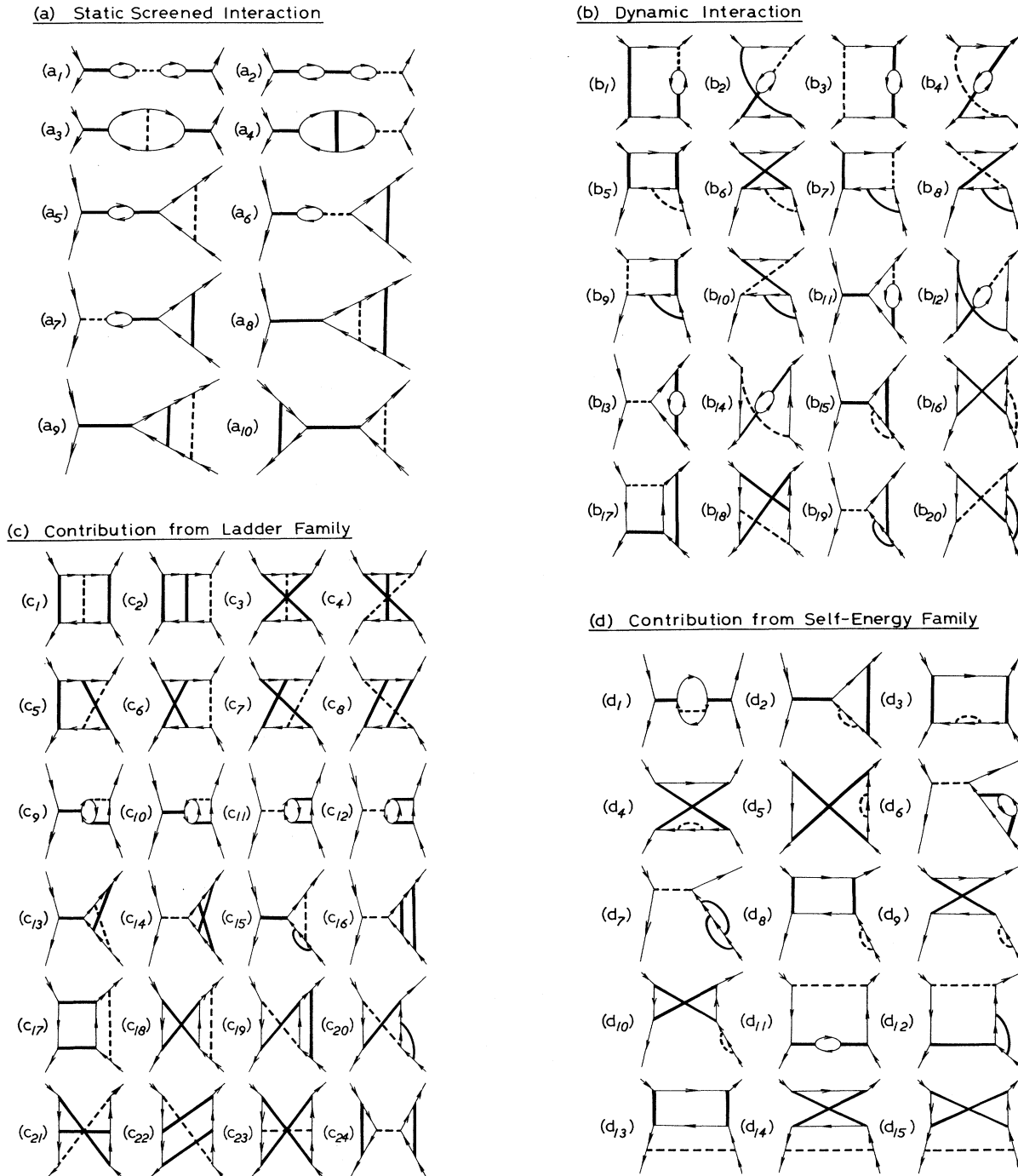


FIG. 4. Second-order terms for  $f_{k\sigma k'\sigma'}$ . The diagrams in (a), (b), (c), and (d) correspond, respectively, to the terms of the static screened interaction, and dynamic interaction in the ring family, the interaction from the ladder family, and that from the self-energy family.

different from those of the ring and ladder families. In Fig. 4(d) we show the terms in  $f_{\mathbf{k}\sigma\mathbf{k}'\sigma'}^{(2;s)}$ , which can be classified into three. The diagrams (d<sub>1</sub>)–(d<sub>5</sub>) belong to  $I_{\mathbf{k}\sigma\mathbf{k}'\sigma'}$ . They give corrections to the first-order terms by the insertion of the self-energy correction to the internal electron line. The diagrams (d<sub>6</sub>)–(d<sub>10</sub>) give the effect of the renormalization factor  $z$  by the insertion of the self-

energy correction to the external electron line, while those of (d<sub>11</sub>)–(d<sub>15</sub>) are examples of the second diagram of the integral equation for  $f_{\mathbf{k}\sigma\mathbf{k}'\sigma'}$  in Fig. 1.

A very important cancellation works between the diagrams in the second and third classes. For instance, the sum of the diagrams (d<sub>6</sub>), (d<sub>7</sub>), (d<sub>11</sub>), and (d<sub>12</sub>) is obtained as

$$f_{\mathbf{k}\sigma\mathbf{k}'\sigma'}^{(2;s;d_6)} + f_{\mathbf{k}\sigma\mathbf{k}'\sigma'}^{(2;s;d_7)} + f_{\mathbf{k}\sigma\mathbf{k}'\sigma'}^{(2;s;d_{11})} + f_{\mathbf{k}\sigma\mathbf{k}'\sigma'}^{(2;s;d_{12})} = \delta_{\sigma\sigma'} \sum_{\mathbf{q}} \sum_{\mathbf{p},\tau} \bar{V}_s(q) [\bar{V}(|\mathbf{k}'-\mathbf{k}|) - \bar{V}(|\mathbf{k}'-\mathbf{k}-\mathbf{q}|)]$$

$$\times \left[ \left[ \bar{V}_s(q)\epsilon(q,0) - \delta_{\sigma\tau} \bar{V}_s(|\mathbf{k}+\mathbf{p}+\mathbf{q}|) \right] \frac{(1-n_{\mathbf{k}+\mathbf{q},\sigma})n_{\mathbf{p}\tau}(1-n_{\mathbf{p}+\mathbf{q},\tau})}{(\epsilon_{\mathbf{p}+\mathbf{q}}-\epsilon_{\mathbf{p}}+\epsilon_{\mathbf{k}+\mathbf{q}}-\epsilon_F)^2} \right.$$

$$\left. + [\bar{V}_s(q)\epsilon(q,0) - \delta_{\sigma\tau} \bar{V}_s(|\mathbf{p}-\mathbf{k}|)] \frac{n_{\mathbf{k}+\mathbf{q},\sigma}n_{\mathbf{p}\tau}(1-n_{\mathbf{p}+\mathbf{q},\tau})}{(\epsilon_{\mathbf{p}+\mathbf{q}}-\epsilon_{\mathbf{p}}-\epsilon_{\mathbf{k}+\mathbf{q}}+\epsilon_F)^2} \right] + (\mathbf{k} \leftrightarrow \mathbf{k}'). \quad (3.7)$$

In (3.7) the sum of  $f_{\mathbf{k}\sigma\mathbf{k}'\sigma'}^{(2;s;d_6)}$  and  $f_{\mathbf{k}\sigma\mathbf{k}'\sigma'}^{(2;s;d_7)}$  is given by the terms proportional to  $\bar{V}(|\mathbf{k}'-\mathbf{k}|)$ . The sum divided by  $-\bar{V}(|\mathbf{k}'-\mathbf{k}|)$  is just twice the second-order contribution to  $z$ , which was calculated from the magnitude of the discontinuity of the momentum distribution function in the interacting system in Ref. 3. Since the deviation of  $z$  from 1 is not small in the electron gas at metallic densities,<sup>3</sup> the sum of  $f_{\mathbf{k}\sigma\mathbf{k}'\sigma'}^{(2;s;d_6)}$  and  $f_{\mathbf{k}\sigma\mathbf{k}'\sigma'}^{(2;s;d_7)}$  is by no means small. However, their contribution is almost canceled by that of  $f_{\mathbf{k}\sigma\mathbf{k}'\sigma'}^{(2;s;d_{11})}$  and  $f_{\mathbf{k}\sigma\mathbf{k}'\sigma'}^{(2;s;d_{12})}$  given by the terms proportional to  $\bar{V}(|\mathbf{k}'-\mathbf{k}-\mathbf{q}|)$  in (3.7). The same situation also occurs in other orders. For example, in zeroth order, the term in Fig. 2(c<sub>1</sub>) is almost canceled by that in Fig. 2(c<sub>2</sub>). The present observation suggests that it is a sensible approximation to neglect the second diagram in Fig. 1 together with  $z$  fixed to 1 in the calculation of  $f_{\mathbf{k}\sigma\mathbf{k}'\sigma'}$ , as is often employed without any justification.<sup>20,21,33</sup> In other words, if the effect of the deviation of  $z$  from 1 in the microscopic calculation of  $f_{\mathbf{k}\sigma\mathbf{k}'\sigma'}$  is included, we also have to consider the corresponding terms in the second diagram in Fig. 1. Without those terms the inclusion of  $z$  will not result in the improvement.

### F. Higher-order terms

Up to second order we can perform all the multidimensional integrals in the terms for  $f_{\mathbf{k}\sigma\mathbf{k}'\sigma'}$  rather accurately by the Gauss quadrature procedure even at the present level of computer technology. However, it is not possible to do the same for the terms higher than second order. Fortunately, we know from the calculation of the ground-state properties that only the ring family up to sixth order as given in (B1)–(B3) in I needs to be considered for the electron gas at metallic densities. As in second order, we can divide the contribution of the higher-order ring family into two parts. The primary part is composed of the terms in the static screened interaction which is a direct extension of  $f_{\mathbf{k}\sigma\mathbf{k}'\sigma'}^{(2;rs)}$  to higher orders. We can obtain those terms explicitly by taking

the derivatives of  $n_{\mathbf{k}_i\sigma_i}(1-n_{\mathbf{k}_i+\mathbf{q},\sigma_i})$  successively with respect to  $n_{\mathbf{k}\sigma}$  and  $n_{\mathbf{k}'\sigma'}$  in the energy expressions (B1)–(B3) in I. The multidimensional integrals in those terms can be performed up to sixth order.

The other part is the dynamic interaction. The multidimensional integrals in those terms are as difficult as those in the contribution from the ladder diagrams. Thus we cannot obtain accurate values for them even in fourth order. However, an estimate of those terms indicates that the contributions of the dynamic interaction in higher orders are small in the electron gas at metallic densities. Therefore, we neglect those contributions in this paper.

## IV. CALCULATED RESULTS

### A. Basic relations

Landau derived the formulas for the effective mass  $m^*$ , compressibility  $\kappa$ , and spin susceptibility  $\chi$  as<sup>4</sup>

$$m/m^* = 1 - F_1^{\uparrow\uparrow} - F_1^{\uparrow\downarrow}, \quad (4.1)$$

$$\kappa_F/\kappa = m/m^* + F_0^{\uparrow\uparrow} + F_0^{\uparrow\downarrow}, \quad (4.2)$$

and

$$\chi_F/\chi = m/m^* + F_0^{\uparrow\uparrow} - F_0^{\uparrow\downarrow}, \quad (4.3)$$

where  $\kappa_F$  and  $\chi_F$  are the values of  $\kappa$  and  $\chi$  in the noninteracting system, and the Landau parameter  $F_l^{\sigma\sigma'}$  for  $l=0$  and 1 is defined as

$$F_l^{\sigma\sigma'} = \sum_{\mathbf{k}'} \delta(\epsilon_{\mathbf{k}'} - \epsilon_F) \left[ \frac{\mathbf{k} \cdot \mathbf{k}'}{k_F^2} \right]^l f_{\mathbf{k}\sigma\mathbf{k}'\sigma'}, \quad (4.4)$$

with  $|\mathbf{k}|=k_F$ . In accordance with the expansion of the Landau interaction function into components such as  $f_{\mathbf{k}\sigma\mathbf{k}'\sigma'}^{(0;rs)}$ , we can define the corresponding expansion of the Landau parameters by (4.4). We denote the components by expressions such as  $F_l^{\sigma\sigma'}(0;rs)$ .



### B. Landau parameters

In Fig. 5 we show the calculated results of all the components of the Landau parameters  $F_l^{\sigma\sigma'}$  up to second order as a function of  $r_s$ . For the spin-parallel parts [Figs. 5(a) and 5(b)], the components of the static screened interaction dominate others. In particular,  $F_l^{\uparrow\uparrow}(1:rs)$  always gives by far the largest contribution. Since the absolute value of  $F_l^{\uparrow\uparrow}(2:rs)$  is about a half of that of  $F_l^{\uparrow\uparrow}(1:rs)$ , we can see that the expansion of the static

screened interaction has a tendency to converge. However, the value of  $F_l^{\uparrow\uparrow}(2:rs)$  is too large to neglect the higher-order components of the static screened interaction. On the other hand, the higher-order contributions of the ladder terms and the dynamic interaction in the ring family can be neglected, partly because the absolute values of those terms are small even in second order and partly because they tend to cancel to one another especially for  $F_0^{\uparrow\uparrow}$ . The second-order self-energy contribution  $F_0^{\uparrow\uparrow}(2:s)$  is rather large primarily because of the term in

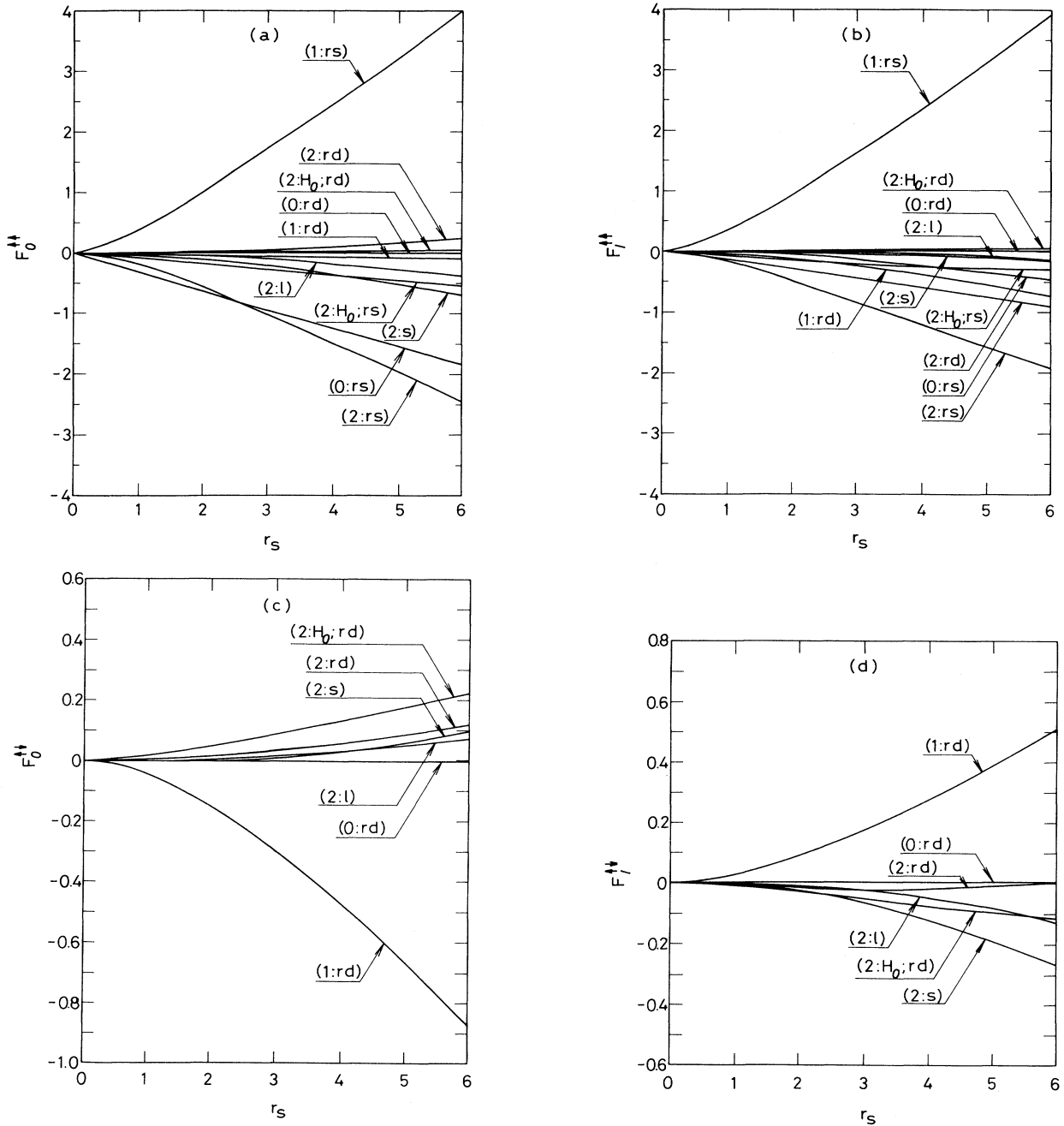


FIG. 5. Landau parameters as a function of  $r_s$  in the definition of (4.4). The cases of (a) and (b) treat the spin-parallel parts, while those of (c) and (d) the spin-antiparallel ones. All the components up to second order are shown. Note that the curve represented by, for example, (1:rs) in (a) gives the results of  $F_0^{\uparrow\uparrow}(1:rs)$ .

Fig. 4(d<sub>1</sub>). Since the self-energy terms as well as the  $H_0$  ones are present only in even-power orders, the next-order terms are in fourth order. Among the contributions from the fourth-order self-energy family given in (B4) in I, we have tentatively evaluated the terms having a structure similar to that in Fig. 4(d<sub>1</sub>) and found that their sum is small. Thus the higher-order self-energy contributions will not be considered.

For the spin-antiparallel parts, there is no contribution from the static screened interaction. Thus we anticipate that a convergent result for  $F_l^{\uparrow\downarrow}$  can be obtained even by the calculation up to second order. The results in Figs. 5(c) and 5(d) show clearly the correctness of the anticipation. The largest contribution comes from  $F_l^{\uparrow\downarrow}(1:rd)$  whose absolute value is only about one-fifth of that of  $F_l^{\uparrow\downarrow}(1:rs)$ . We can also see the rapid convergence by comparing the values of the second-order terms with  $F_l^{\uparrow\downarrow}(1:rd)$ .

In Fig. 6 we plot our results for  $\kappa_F/\kappa$ ,  $\chi_F/\chi$ , and  $m/m^*$  as a function of  $r_s$ . The dashed curves represent the results with the Landau parameters summed up to second order, while the dot-dashed and solid curves show, respectively, those with the contributions from the static screened interaction up to fourth and sixth orders, in addition to the components of the Landau parameters in Fig. 5. Because the component of the static screened

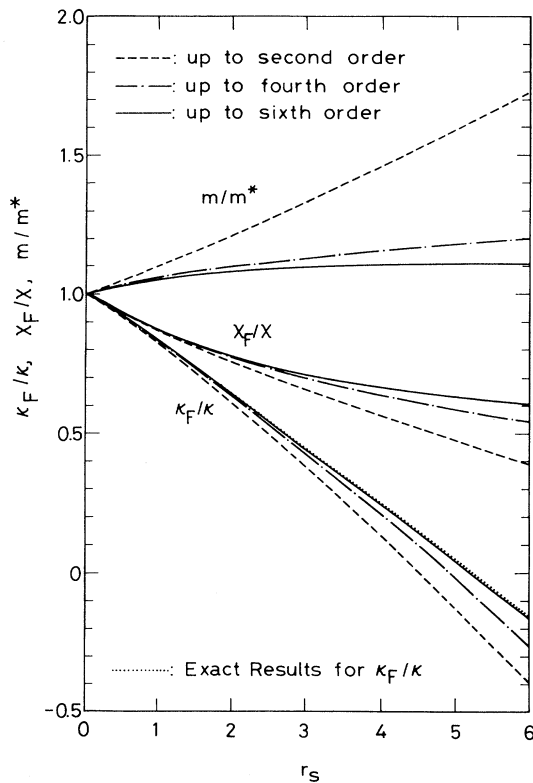


FIG. 6. Our results for  $\kappa_F/\kappa$ ,  $\chi_F/\chi$ , and  $m/m^*$  as a function of  $r_s$ . The dashed curves represent the results up to second order, while the dot-dashed and solid curves show, respectively, those with the contributions from the static screened interaction up to fourth and sixth orders.

interaction in  $F_l^{\uparrow\downarrow}$  is canceled rather strongly by that in  $F_0^{\uparrow\downarrow}$ , we have smaller changes in  $\kappa_F/\kappa$  and  $\chi_F/\chi$  than that in  $m/m^*$  with the increase of the order. We have made rough estimates of the contributions from the seventh- and eighth-order components of the static screened interaction and find that those contributions will make changes for the results in Fig. 6 by at most a few percent. Thus the values given by the solid curves in Fig. 6 may be regarded as our final results. In order to make an independent check of the validity of our procedure, we also show the exact results<sup>9,16</sup> for  $\kappa_F/\kappa$  by the dotted curve in Fig. 6. Those exact results are obtained from the thermodynamic relation as explained, for example, in (5.2) in I. By comparing our results for  $\kappa_F/\kappa$ , including all the four values of  $F_l^{\sigma\sigma'}$  with the exact ones, we are confident that our procedure works quite well.

Since the exact values are known, we need not discuss  $\kappa_F/\kappa$  any more. However, we do not know the exact values of either the spin susceptibility or effective mass. Thus we have to make a detailed discussion of them.

### C. Spin susceptibility

In Fig. 7 we plot the results of  $\chi_F/\chi$  as a function of  $r_s$  in various approaches. For comparison, we show the re-

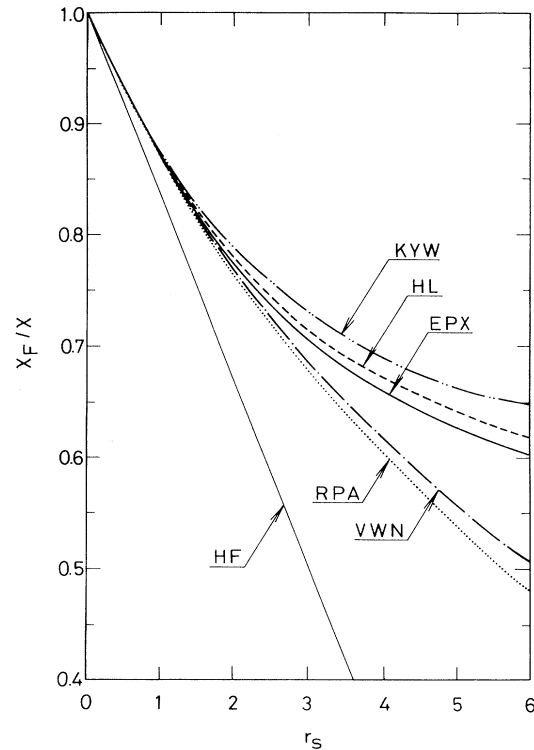


FIG. 7. Results of  $\chi_F/\chi$  as a function of  $r_s$  in various approaches. The solid, thin-solid, dotted, dashed, dot-dashed, and double-dot-dashed curves give, respectively, the results in the EPX, the Hartree-Fock approximation (HF), the RPA, the approach of Hedin and Lundqvist (HL) (Ref. 10), that of Vosko, Wilk, and Nusair (VWN) (Ref. 9), and that of Kawazoe, Yasuhara, and Watabe (KYW) (Ref. 34).

sults in the Hartree-Fock approximation (HF) and RPA by the thin solid line and dotted curve, respectively. Vosko, Wilk, and Nusair<sup>9</sup> (VWN) obtained the results by the thermodynamic relation with the total energies of the spin-polarized electron gas, which were estimated by an interpolation scheme. Their results are given by the dot-dashed curves. Somewhat old results of Hedin and Lundqvist<sup>10</sup> (HL) are shown by the dashed curve. The results of Rice<sup>20</sup> are about the same as those of HL. The double-dot-dashed curve gives the results of Kawazoe, Yasuhara, and Watabe<sup>34</sup> (KYW). Their values for  $\chi$  are probably the smallest among the significant calculations. Our results indicated by EPX are given by the solid curve.

In 1976, Kushida, Murphy, and Hanabusa<sup>35</sup> summarized the values for  $\chi$  in the electron gas in quite many theoretical approaches. They found that there was a "consensus" curve in the  $(r_s, \chi)$  plane among those many theoretical results. They also found that the experimental results in the alkali metals agreed with the values on the consensus curve. Since the results of VWN are virtually on the consensus curve, most people believe that their results are, if not exact, very close to the exact values.<sup>36</sup> In our opinion, however, their results are not so reliable. It is true that there is a definite difference between their values and those in the RPA in Fig. 7. The difference, however, originates entirely from that in  $\kappa_F/\kappa$ . We cannot find any difference between the values of VWN and those in the RPA in the essential part, namely,  $F_0^{\uparrow\downarrow}$ , as we shall show in the following way. Combining (4.2) with (4.3), we can determine the values of  $F_0^{\uparrow\downarrow}$  in the approach of VWN through

$$F_0^{\uparrow\downarrow} = \frac{1}{2} \left[ \frac{\kappa_F}{\kappa} - \frac{\chi_F}{\chi} \right], \quad (4.5)$$

with the tabulated values for  $\kappa_F/\kappa$  and  $\chi_F/\chi$  in Ref. 36. The values obtained for  $F_0^{\uparrow\downarrow}$  are plotted in Fig. 8 by the dot-dashed curve, but they agree with the results in the RPA (dotted curve),  $F_0^{\uparrow\downarrow}$  (RPA), at least up to two digits and often even three. We have calculated  $F_0^{\uparrow\downarrow}$  (RPA) by (4.4) with the Landau interaction function given by (3.1) with the replacement of  $\tilde{V}_l(q)$  by  $V(q)$ . Namely,  $F_0^{\uparrow\downarrow}$  (RPA) is given by

$$F_0^{\uparrow\downarrow}(\text{RPA}) = -\frac{\alpha^2 r_s^2}{2\pi^3} \int_0^\infty dz z^3 \times \int_0^\infty du \frac{[Q(z, u)]^2}{[z^2 + (\alpha r_s / \pi) P(z, u)]^2}, \quad (4.6)$$

with

$$Q(z, u) = \frac{1}{2z} \ln \left[ \frac{u^2 + (1+z)^2}{u^2 + (1-z)^2} \right], \quad (4.7)$$

and

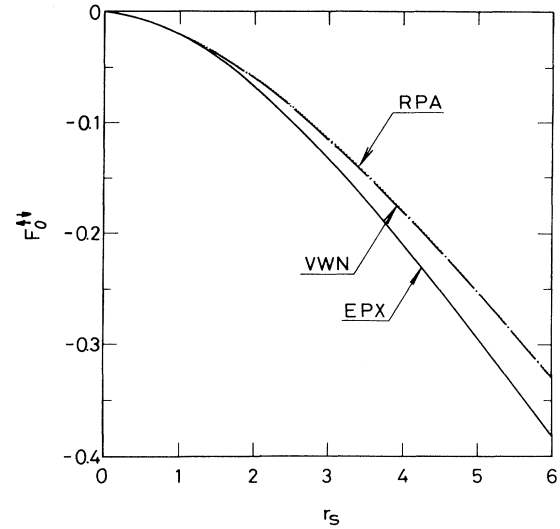


FIG. 8. Results for  $F_0^{\uparrow\downarrow}$  as a function of  $r_s$ . The solid curve gives those in the EPX through (4.4), while the dotted one represents those in the RPA through (4.6). The dot-dashed curve shows the results of Vosko, Wilk, and Nusair (VWN) (Ref. 9) through (4.5).

$$P(z, u) = \frac{1}{2} \left[ 1 + \frac{1-z^2+u^2}{2} Q(z, u) - u \tan^{-1} \left[ \frac{2u}{u^2+z^2-1} \right] \right]. \quad (4.8)$$

We can see clearly from (4.6) that  $F_0^{\uparrow\downarrow}$  (RPA) is negative definite, but the exact values for  $F_0^{\uparrow\downarrow}$  should be even smaller than those for  $F_0^{\uparrow\downarrow}$  (RPA). We believe that those exact values are very close to our values indicated by EPX (the solid curve in Fig. 8). This is because for the processes of the momentum transfer  $q$  of the order of  $k_F$  [or  $z \approx \frac{1}{2}$  in (4.6)], the actual interaction between electrons with antiparallel spins becomes much stronger than the effective potential in the RPA if we consider the effect of the vertex corrections. In real-space representation the same can be stated, that the screening effect does not work so effectively as in the RPA between electrons with short-range separation. In this way  $F_0^{\uparrow\downarrow}$  (RPA) should be the upper limit for the true  $F_0^{\uparrow\downarrow}$ . Combining the above fact with (4.5) and using the exact values for  $\kappa_F/\kappa$ , we have a firm statement that the results of VWN for  $\chi_F/\chi$  give the lower bound. Probably the exact values for  $\chi_F/\chi$  in the electron gas lie close to our results.

#### D. Effective mass

The effective mass is an even more controversial quantity than the spin susceptibility. In Fig. 9 we show the results for  $m^*/m$  as a function of  $r_s$  in the RPA, Hedin's approach,<sup>11</sup> and the EPX method together with the recent results of Yasuhara and Ousaka<sup>33</sup> (YO) by the dotted, dashed, solid, and dot-dashed curves, respectively. Before the appearance of YO, all the significant calcula-

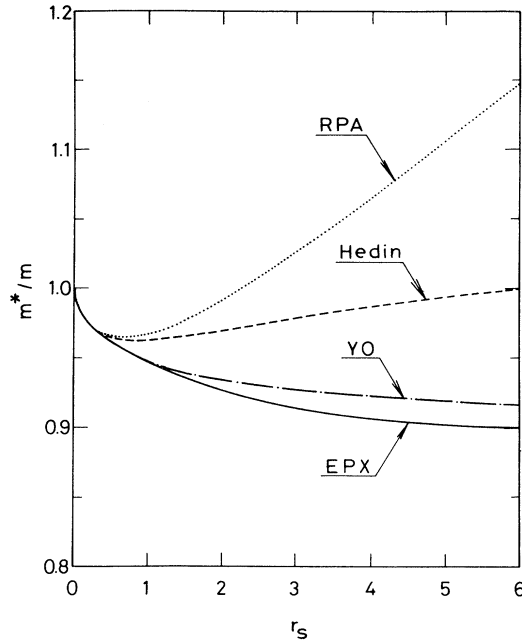


FIG. 9. Results for  $m^*/m$  as a function of  $r_s$  in the EPX, the RPA, the approach of Hedin (Ref. 11), and that of Yasuhara and Ousaka (YO) (Ref. 33). They are, respectively, represented by the solid, dotted, dashed, and dot-dashed curves.

tions had a tendency as in the RPA. Namely,  $m^*/m$  decreases first and then increases with the increase of  $r_s$ . The experimental values in the alkali metals seem to agree with this behavior. However, the exact behavior of  $m^*/m$  in the electron gas is not necessarily the same as the experimental one even in such metals. Yasuhara and Ousaka discussed the incorrectness of the behavior obtained in the RPA and its refinement<sup>20</sup> in detail.<sup>21,33,37</sup> Thus we do not repeat the discussion here. We only mention that our present calculation gives support to their results. There is a small discrepancy between our results and those of YO, but the difference is about the same as the magnitude of uncertainty caused by the neglect of many higher-order terms in our approach. Thus, at present, we cannot say whether the difference is significant or not. As for the monotonic behavior of  $m^*/m$  as a function of  $r_s$ , we have rather strong confidence in the correctness of the behavior mainly because the second-order calculation has such a tendency. We have the experience that the calculations up to

second order always give at least qualitatively correct behavior as a function of  $r_s$  for all the quantities so far calculated for the ground-state properties.

Finally, we note that the monotonic behavior of  $m^*/m$  is not always true for the multivalley electron gas. In fact, as we have shown in I, the RPA gives a very accurate description for the valley degeneracy  $g_v$  larger than about 4 at metallic densities. Thus, for such a situation,  $m^*/m$  behaves in much the same way as given by the dotted curve in Fig. 9.

## V. SUMMARY AND DISCUSSION

In a previous paper<sup>38</sup> we made an extension of the EPX method to treat the finite-temperature problem, while in this paper an extension is given to describe the low-lying excited states of an interacting many-fermion system. In particular, a microscopic representation for Landau's Fermi-liquid parameter is provided. The general framework is applied to the electron gas at metallic densities to calculate quasiparticle properties such as the compressibility  $\kappa$ , spin susceptibility  $\chi$ , and effective mass  $m^*$ . The results obtained for  $\kappa$  are very close to the exact values. The same situation is expected to occur in both  $\chi$  and  $m^*$ , though at present we do not have the exact values for those quantities to compare with.

In the RPA the results for both  $\chi$  and  $m^*$  in the electron gas are in rather good agreement with the experimental ones in the alkali metals which have been considered as the best candidate for the electron-gas model. However, recent elaborate calculations including the present one in the EPX method suggest that there is a considerable difference between the results in the RPA and the exact ones. Thus we have to reconsider the applicability of the electron-gas model even to the alkali metals. In fact, this is one of the motivations to develop the EPX method as mentioned in Sec. I. Probably the main issue in real solids is the interplay of many-body effects with the Hartree potential, which is absent in the electron-gas model. There might be some mechanism in alkali metals which validates the use of the RPA even for the short-range correlation.

## ACKNOWLEDGMENTS

The author would like to thank H. Yasuhara for useful discussions at the final stage of this research.

<sup>1</sup>Y. Takada, Phys. Rev. A **28**, 2417 (1983).

<sup>2</sup>Y. Takada, Phys. Rev. B **35**, 6923 (1987).

<sup>3</sup>Y. Takada and H. Yasuhara (unpublished).

<sup>4</sup>L. D. Landau, Zh. Eksp. Teor. Fiz. **30**, 1058 (1956) [Sov. Phys.—JETP **3**, 920 (1957)].

<sup>5</sup>P. Hohenberg and W. Kohn, Phys. Rev. **136**, B864 (1964); W. Kohn and L. J. Sham, Phys. Rev. **140**, A1133 (1965); W. Kohn and P. Vashishta, in *Theory of the Inhomogeneous Electron Gas*, edited by S. Lundqvist and N. H. March (Plenum, New York, 1983), p. 79.

<sup>6</sup>Excellent reviews are given in Chap. 1 of *Many-Body Phenomena at Surfaces*, edited by D. Langreth and H. Suhl (Academic, Orlando, 1984).

<sup>7</sup>In this respect, see, for example, K. T. Park, K. Terakura, T. Oguchi, A. Yanase, and M. Ikeda, J. Phys. Soc. Jpn. **57**, 3445 (1988).

<sup>8</sup>D. M. Ceperley and B. J. Alder, Phys. Rev. Lett. **45**, 566 (1980).

<sup>9</sup>S. H. Vosko, L. Wilk, and M. Nusair, Can. J. Phys. **58**, 1200 (1980).

- <sup>10</sup>L. Hedin and S. Lundqvist, in *Solid State Physics*, edited by F. Seitz, D. Turnbull, and H. Ehrenreich (Academic, New York, 1969), Vol. 23, p. 1.
- <sup>11</sup>L. Hedin, Phys. Rev. **139**, A796 (1965).
- <sup>12</sup>A. H. MacDonald, M. W. C. Dharma-wardana, and D. J. W. Geldart, J. Phys. F **10**, 1719 (1980); A. H. MacDonald, *ibid.* **10**, 1737 (1980).
- <sup>13</sup>J. E. Northrup, M. S. Hybertsen, and S. G. Louie, Phys. Rev. B **39**, 8198 (1989).
- <sup>14</sup>See, for example, A. L. Fetter and J. D. Walecka, *Quantum Theory of Many-Particle Systems* (McGraw-Hill, New York, 1971).
- <sup>15</sup>M. Gell-Mann and K. Brueckner, Phys. Rev. **106**, 364 (1957).
- <sup>16</sup>Y. Takada, preceding paper, Phys. Rev. B **43**, 5962 (1991).
- <sup>17</sup>K. S. Singwi and M. P. Tosi, in *Solid State Physics*, edited by H. Ehrenreich, F. Seitz, and D. Turnbull (Academic, New York, 1981), Vol. 36, p. 177; S. Ichimaru, Rev. Mod. Phys. **54**, 1017 (1982).
- <sup>18</sup>C. A. Kukkonen and J. W. Wilkins, Phys. Rev. B **19**, 6075 (1979); C. A. Kukkonen and A. W. Overhauser, *ibid.* **20**, 550 (1979); G. Vignale and K. S. Singwi, *ibid.* **32**, 2156 (1985).
- <sup>19</sup>T. K. Ng and K. S. Singwi, Phys. Rev. B **34**, 7738 (1986); **34**, 7743 (1986).
- <sup>20</sup>T. M. Rice, Ann. Phys. (N.Y.) **31**, 100 (1965).
- <sup>21</sup>H. Yasuhara, Y. Ousaka, and H. Suehiro, J. Phys. C **20**, 2511 (1987).
- <sup>22</sup>J. M. Luttinger and P. Nozières, Phys. Rev. **127**, 1423 (1962); **127**, 1431 (1962).
- <sup>23</sup>R. Jastrow, Phys. Rev. **98**, 1479 (1955).
- <sup>24</sup>D. Ceperley, Phys. Rev. B **18**, 3216 (1978).
- <sup>25</sup>S. Fahy, X. W. Wang, and S. G. Louie, Phys. Rev. Lett. **61**, 1631 (1988).
- <sup>26</sup>L. J. Lantto, Phys. Rev. B **22**, 1380 (1980).
- <sup>27</sup>J. G. Zabolitzky, Phys. Rev. B **22**, 2353 (1980).
- <sup>28</sup>J. W. Clark and E. Feenberg, Phys. Rev. **113**, 388 (1959).
- <sup>29</sup>E. Krotscheck, Ann. Phys. (N.Y.) **155**, 1 (1984).
- <sup>30</sup>M. Gell-Mann, Phys. Rev. **106**, 369 (1957).
- <sup>31</sup>E. Krotscheck and J. W. Clark, Nucl. Phys. **A28**, 73 (1979).
- <sup>32</sup>P. Nozières, *Theory of Interacting Fermi Systems* (Benjamin, New York, 1964).
- <sup>33</sup>H. Yasuhara and Y. Ousaka, Solid State Commun. **64**, 673 (1987).
- <sup>34</sup>Y. Kawazoe, H. Yasuhara, and M. Watabe, J. Phys. C **10**, 3293 (1977).
- <sup>35</sup>T. Kushida, J. C. Murphy, and M. Hanabusa, Phys. Rev. B **13**, 5136 (1976).
- <sup>36</sup>See, for example, N. Iwamoto and D. Pines, Phys. Rev. B **29**, 3924 (1984).
- <sup>37</sup>H. Yasuhara and Y. Ousaka (unpublished).
- <sup>38</sup>Y. Takada and T. Kita, Phys. Rev. A **42**, 3242 (1990).